

Asymmetric two-component Fermi gas with unequal masses

M. Iskin and C. A. R. Sá de Melo

School of Physics, Georgia Institute of Technology, Atlanta, Georgia 30332, USA

(Dated: July 20, 2021)

We analyze the zero temperature phase diagram for an asymmetric two-component Fermi gas as a function of mass anisotropy and population imbalance. We identify regions corresponding to normal, or uniform/non-uniform superfluid phases, and discuss topological quantum phase transitions in the Bardeen-Cooper-Schrieffer (BCS), unitarity and Bose-Einstein condensation (BEC) limits. Lastly, we derive the zero temperature low frequency and long wavelength collective excitation spectrum, and recover the Bogoliubov relation for weakly interacting dilute bosons in the BEC limit.

PACS numbers: 03.75.Ss, 03.75.Hh, 05.30.Fk

The evolution from Bardeen-Cooper-Schrieffer (BCS) to Bose-Einstein condensation (BEC) is a very important topic of current research for the condensed matter, nuclear, atomic and molecular physics communities. Recent advances in atomic physics have allowed for the study of superfluid properties in symmetric two-component fermion superfluids (equal mass and equal population) as a function of scattering length, where the theoretically predicted crossover from BCS to BEC was observed [1, 2].

Since the population of each component as well as the interaction strength between two components are experimentally tunable, these knobs enabled the study of the BCS to BEC evolution in asymmetric two-component fermion superfluids (equal mass but unequal population) [3, 4]. In contrast with the crossover physics found in the symmetric case, these experiments have demonstrated the existence of phase transitions between normal and superfluid phases, as well as phase separation between superfluid (paired) and normal (excess) fermions as a function of population imbalance.

Arguably one of the next frontiers of exploration in cold Fermi gases is the study of asymmetric two-component fermion superfluidity (unequal masses and equal or unequal population) in two-species fermion mixtures from the BCS to the BEC limit. Earlier works on two-species fermion mixtures were limited to the BCS regime [5, 6, 7, 8]. However, very recently, the evolution from BCS to BEC was preliminarily addressed in homogenous systems as a function of population imbalance and scattering length for ${}^6\text{Li}$ and ${}^{40}\text{K}$ mixture [9]. In addition, the superfluid phase diagram of trapped systems at unitarity was also analyzed as a function of population imbalance and mass anisotropy [10].

In this manuscript, we study the BCS to BEC evolution of asymmetric two-component fermion superfluids as a function of population imbalance and mass anisotropy. Our results for a homogeneous system are as follows. We analyze the zero temperature phase diagram for an asymmetric two-component Fermi gas as a function of mass anisotropy and population imbalance. We identify regions corresponding to normal, and uniform or non-

uniform superfluid phases, and discuss topological quantum phase transitions in the BCS, unitarity and BEC limits. Lastly, we derive the zero temperature low frequency and long wavelength collective excitation spectrum, and recover the Bogoliubov relation for weakly interacting dilute bosons in the BEC limit.

To describe a dilute asymmetric two-component Fermi gas in three dimensions, we start from the pseudo-spin singlet Hamiltonian ($\hbar = 1$)

$$H = \sum_{\mathbf{k},\sigma} \xi_{\mathbf{k},\sigma} a_{\mathbf{k},\sigma}^\dagger a_{\mathbf{k},\sigma} + \sum_{\mathbf{k},\mathbf{k}',\mathbf{q}} V(\mathbf{k},\mathbf{k}') b_{\mathbf{k},\mathbf{q}}^\dagger b_{\mathbf{k}',\mathbf{q}}, \quad (1)$$

where the pseudo-spin σ labels the hyperfine states represented by the creation operator $a_{\mathbf{k},\sigma}^\dagger$, and $b_{\mathbf{k},\mathbf{q}}^\dagger = a_{\mathbf{k}+\mathbf{q}/2,\uparrow}^\dagger a_{-\mathbf{k}+\mathbf{q}/2,\downarrow}^\dagger$. Here, $\xi_{\mathbf{k},\sigma} = \epsilon_{\mathbf{k},\sigma} - \mu_\sigma$, where $\epsilon_{\mathbf{k},\sigma} = k^2/(2m_\sigma)$ is the energy and μ_σ is the chemical potential of the fermions. Notice that, we allow for the fermions to have different masses m_σ and different populations controlled by independent chemical potentials μ_σ . The attractive fermion-fermion interaction $V(\mathbf{k},\mathbf{k}')$ can be written in a separable form as $V(\mathbf{k},\mathbf{k}') = -g\Gamma_{\mathbf{k}}^* \Gamma_{\mathbf{k}'}$ where $g > 0$, and $\Gamma_{\mathbf{k}} = 1$ for the s-wave contact interaction considered in this manuscript.

The gaussian effective action for H is $S_{\text{gauss}} = S_0 + (\beta/2) \sum_{\mathbf{q}} \bar{\Lambda}^\dagger(\mathbf{q}) \mathbf{F}^{-1}(\mathbf{q}) \bar{\Lambda}(\mathbf{q})$, where $\mathbf{q} = (\mathbf{q}, v_\ell)$ with bosonic Matsubara frequency $v_\ell = 2\ell\pi/\beta$. Here, $\beta = 1/T$, $\bar{\Lambda}^\dagger(\mathbf{q})$ is the order parameter fluctuation field, and the matrix $\mathbf{F}^{-1}(\mathbf{q})$ is the inverse fluctuation propagator. The saddle point action is

$$S_0 = \beta \frac{|\Delta_0|^2}{g} + \sum_{\mathbf{k}} \left\{ \beta (\xi_{\mathbf{k},+} - E_{\mathbf{k},+}) + \ln[n_F(-E_{\mathbf{k},\uparrow})] + \ln[n_F(-E_{\mathbf{k},\downarrow})] \right\}, \quad (2)$$

where $E_{\mathbf{k},\sigma} = (\xi_{\mathbf{k},+}^2 + |\Delta_{\mathbf{k}}|^2)^{1/2} + s_\sigma \xi_{\mathbf{k},-}$ is the quasiparticle energy when $s_\uparrow = 1$ or the negative of the quasiparticle energy when $s_\downarrow = -1$, and $E_{\mathbf{k},\pm} = (E_{\mathbf{k},\uparrow} \pm E_{\mathbf{k},\downarrow})/2$. Here, $\Delta_{\mathbf{k}} = \Delta_0 \Gamma_{\mathbf{k}}$ is the order parameter, $n_F(E_{\mathbf{k},\sigma})$ is the Fermi distribution and $\xi_{\mathbf{k},\pm} = (\xi_{\mathbf{k},\uparrow} \pm \xi_{\mathbf{k},\downarrow})/2 = k^2/(2m_\pm) - \mu_\pm$, where $m_\pm = 2m_\uparrow m_\downarrow / (m_\downarrow \pm m_\uparrow)$ and $\mu_\pm = (\mu_\uparrow \pm \mu_\downarrow)/2$. Notice that m_+ is twice the reduced

mass of the \uparrow and \downarrow fermions, and that the equal mass case corresponds to $|m_-| \rightarrow \infty$. The fluctuation term in the action leads to a correction to the thermodynamic potential, which can be written as $\Omega_{\text{gauss}} = \Omega_0 + \Omega_{\text{fluct}}$ with $\Omega_0 = S_0/\beta$ and $\Omega_{\text{fluct}} = (1/\beta) \sum_q \ln \det[\mathbf{F}^{-1}(q)/\beta]$.

The saddle point condition $\delta S_0/\delta \Delta_0^* = 0$ leads to an equation for the order parameter

$$\frac{1}{g} = \sum_{\mathbf{k}} \frac{|\Gamma_{\mathbf{k}}|^2}{2E_{\mathbf{k},+}} \mathcal{X}_{\mathbf{k},+}, \quad (3)$$

where $\mathcal{X}_{\mathbf{k},\pm} = (\mathcal{X}_{\mathbf{k},\uparrow} \pm \mathcal{X}_{\mathbf{k},\downarrow})/2$ with $\mathcal{X}_{\mathbf{k},\sigma} = \tanh(\beta E_{\mathbf{k},\sigma}/2)$. As usual, we eliminate g in favor of the scattering length a_F via the relation $1/g = -m_+ V/(4\pi a_F) + \sum_{\mathbf{k}} |\Gamma_{\mathbf{k}}|^2/(2\epsilon_{\mathbf{k},+})$, where $\epsilon_{\mathbf{k},\pm} = (\epsilon_{\mathbf{k},\uparrow} \pm \epsilon_{\mathbf{k},\downarrow})/2$. The order parameter equation has to be solved self-consistently with number equations $N_{\sigma} = -\partial\Omega/\partial\mu_{\sigma}$ which have two contributions $N_{\sigma} = N_{0,\sigma} + N_{\text{fluct},\sigma}$. $N_{0,\sigma}$ is the saddle point number equation given by

$$N_{0,\sigma} = -\frac{\partial\Omega_0}{\partial\mu_{\sigma}} = \sum_{\mathbf{k}} \left(\frac{1 - s_{\sigma}\mathcal{X}_{\mathbf{k},-}}{2} - \frac{\xi_{\mathbf{k},+}}{2E_{\mathbf{k},+}} \mathcal{X}_{\mathbf{k},+} \right) \quad (4)$$

and $N_{\text{fluct},\sigma} = -\partial\Omega_{\text{fluct}}/\partial\mu_{\sigma}$ is the fluctuation contribution to N given by $N_{\text{fluct},\sigma} = -(1/\beta) \sum_q \{\partial[\det \mathbf{F}^{-1}(q)]/\partial\mu_{\sigma}\}/\det \mathbf{F}^{-1}(q)$.

In order to analyze the phase diagram at $T = 0$, we solve the saddle point self-consistency (order parameter and number) equations as a function of population imbalance $P = N_-/N_+$ and mass anisotropy $m_r = m_{\uparrow}/m_{\downarrow}$. Here, $N_{\pm} = (N_{\uparrow} \pm N_{\downarrow})/2$ corresponding to the following momenta $k_{F,\pm}^3 = (k_{F,\uparrow}^3 \pm k_{F,\downarrow}^3)/2$. In addition, we check the stability of saddle point solutions for the uniform superfluid phase using two criteria. The first criterion requires that the curvature $\partial^2\Omega_0/\partial\Delta_0^2$ of the saddle point thermodynamic potential Ω_0 with respect to the saddle point parameter Δ_0 to be positive, where

$$\frac{\partial^2\Omega_0}{\partial\Delta_0^2} = \sum_{\mathbf{k}} |\Delta_{\mathbf{k}}|^2 \left(\frac{\mathcal{X}_{\mathbf{k},+}}{E_{\mathbf{k},+}^3} - \beta \frac{\mathcal{Y}_{\mathbf{k},+}}{2E_{\mathbf{k},+}^2} \right). \quad (5)$$

Here, $\mathcal{Y}_{\mathbf{k},\pm} = (\mathcal{Y}_{\mathbf{k},\uparrow} \pm \mathcal{Y}_{\mathbf{k},\downarrow})/2$ with $\mathcal{Y}_{\mathbf{k},\sigma} = \text{sech}^2(\beta E_{\mathbf{k},\sigma}/2)$. When $\partial^2\Omega_0/\partial\Delta_0^2$ is negative, the uniform saddle point solution does not correspond to a minimum of Ω_0 , and a non-uniform superfluid phase is favored. This criterion is related to the positive definiteness criterion on the compressibility matrix κ with elements $\kappa_{\sigma,\sigma'} = -\partial^2\Omega_0/(\partial\mu_{\sigma}\partial\mu_{\sigma'})$. The second criterion requires that the superfluid density

$$\rho_0(T) = m_{\uparrow}N_{\uparrow} + m_{\downarrow}N_{\downarrow} - \frac{\beta}{6} \sum_{\mathbf{k}} k^2 \mathcal{Y}_{\mathbf{k},+} \quad (6)$$

to be positive. When $\rho_0(T)$ is negative, a spontaneously generated gradient of the phase of the order parameter appears, leading to a non-uniform superfluid phase.

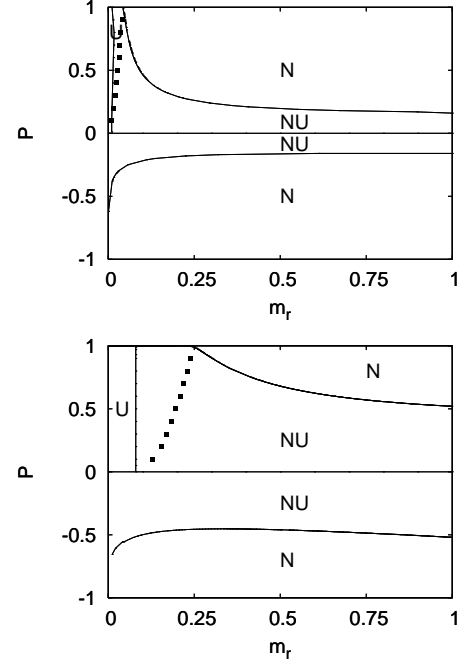


FIG. 1: Phase diagram of $P = (N_{\uparrow} - N_{\downarrow})/(N_{\uparrow} + N_{\downarrow})$ versus $m_r = m_{\uparrow}/m_{\downarrow}$ on the BCS side when a) $1/(k_{F,+}a_F) = -1$ and b) $1/(k_{F,+}a_F) = -0.25$.

Based on these two criteria, we construct the P versus m_r phase diagram for five sets of interaction strengths: $1/(k_{F,+}a_F) = -1$ and -0.25 on the BCS side shown in Fig. 1; $1/(k_{F,+}a_F) = 0$ at unitarity shown in Fig. 2; and $1/(k_{F,+}a_F) = 0.25$ and 1 on the BEC side shown in Fig. 3. In these diagrams, the \uparrow (\downarrow) label always corresponds to lighter (heavier) mass such that lighter (heavier) fermions are in excess when $P > 0$ ($P < 0$). Notice that this choice spans all possible population imbalances and mass ratios. In Figs. 1-3, we indicate the regions of normal (N), and non-uniform (NU) or uniform (U) superfluid phases. The normal phase is characterized by a vanishing order parameter ($\Delta_0 = 0$), while the uniform superfluid phase is characterized by $\rho_0(0) > 0$ and $\partial^2\Omega_0/\partial\Delta_0^2 > 0$. The non-uniform superfluid phase is characterized by $\rho_0(0) < 0$ and/or $\partial^2\Omega_0/\partial\Delta_0^2 < 0$, and it should be of the LOFF-type having one wavevector modulation only near the BCS limit, although closer to unitarity, we expect the non-uniform phase to be substantially different from the LOFF phases having spatial modulation that would encompass several wavevectors. However, from numerical calculations, the first criterion seems to be dominant for all parameter space and the non-uniform superfluid phase is characterized by $\partial^2\Omega_0/\partial\Delta_0^2 < 0$, which indicates possibly phase separation.

We also identify a topological quantum phase transition, which is shown as dotted lines in Figs 1-3. These phases are characterized by the number of zeros of $E_{\mathbf{k},\uparrow}$

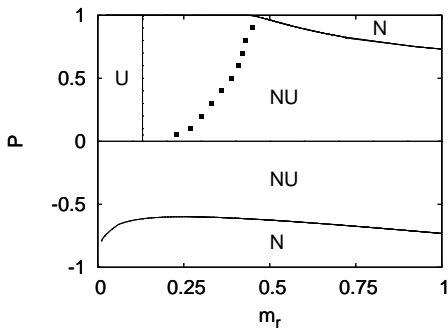


FIG. 2: Phase diagram of $P = (N_\uparrow - N_\downarrow)/(N_\uparrow + N_\downarrow)$ versus $m_r = m_\uparrow/m_\downarrow$ at the unitarity when $1/(k_{F,+}a_F) = 0$.

and $E_{\mathbf{k},\downarrow}$ (zero energy surfaces in momentum space) such that I) $E_{\mathbf{k},\sigma}$ has no zeros and $E_{\mathbf{k},-\sigma}$ has only one, and II) $E_{\mathbf{k},\sigma}$ has no zeros and $E_{\mathbf{k},-\sigma}$ has two zeros. Phase I (II) always appears to the left (right) of the dotted lines. Notice that, the $P = 0$ limit corresponds to case III, where $E_{\mathbf{k},\sigma}$ has no zeros and is always positive. The transition from case II to case I occurring at the dotted lines is quantum in nature, and signatures of it could still be observed at finite temperatures through the measurement of momentum distributions [9]. However, phase II seems to lie always in the NU region and may not be accessible experimentally.

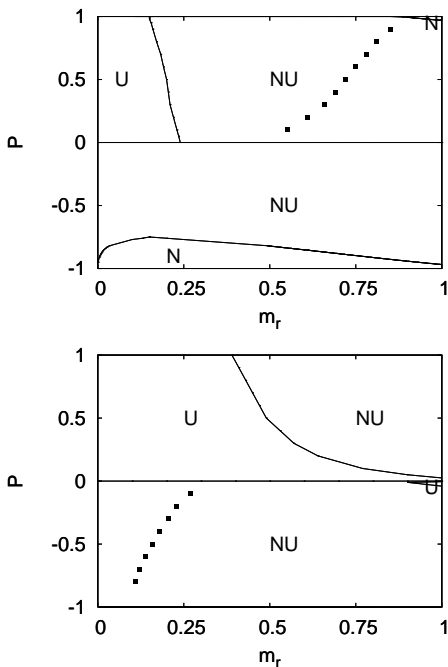


FIG. 3: Phase diagram of $P = (N_\uparrow - N_\downarrow)/(N_\uparrow + N_\downarrow)$ versus $m_r = m_\uparrow/m_\downarrow$ on the BEC side when a) $1/(k_{F,+}a_F) = 0.25$ and b) $1/(k_{F,+}a_F) = 1$.

As shown in Fig. 1a, we find a small region of uniform superfluidity on the BCS side for $1/(k_{F,+}a_F) = -1$

only when the mass anisotropy is small and the lighter fermion are in excess ($P > 0$). Thus, mixtures consisting of ${}^6\text{Li}$ and ${}^{40}\text{K}$ ($m_r \approx 0.15$) or ${}^6\text{Li}$ and ${}^{87}\text{Sr}$ ($m_r \approx 0.07$) are good candidates for future experiments. In the rest of the phase diagram, we find a quantum phase transition from the non-uniform superfluid to the normal phase beyond a critical population imbalance for both positive and negative P . The phase space of uniform superfluidity expands while that of the normal phase shrinks with increasing interaction strength as shown in Fig. 1b.

This general trend continues into the unitarity limit [$1/(k_{F,+}a_F) = 0$] as shown in Fig. 2. Since this limit is theoretically important as well as experimentally accessible, we suggest that Fermi mixtures corresponding to $0 < m_r < 0.45$ have phase diagrams which are qualitatively different from those of $0.45 < m_r < 1$ as a function of P . Thus, mixtures consisting of ${}^6\text{Li}$ and ${}^2\text{H}$ ($m_r \approx 0.33$), ${}^6\text{Li}$ and ${}^{25}\text{Mg}$ ($m_r \approx 0.24$) or ${}^{40}\text{K}$ and ${}^{87}\text{Sr}$ ($m_r \approx 0.64$) are also good candidates for future experiments. Notice that, our results for the case of equal masses ($m_r = 1$) are in close agreement with recent MIT experiments [3] in a trap. At unitarity, our non-uniform superfluid to normal state boundary occurs at $P \approx \pm 0.73$, and the MIT group obtains $P \approx \pm 0.70(4)$ for their superfluid to normal boundary.

Additional increase of interaction strength beyond unitarity on the BEC side leads to further expansion (shrinkage) of the uniform superfluid (normal) region as shown in Fig. 3. When heavier fermions are in excess ($P < 0$), a uniform superfluid phase is not possible for any mass anisotropy until a critical interaction strength is reached. The critical interaction strength corresponds to $1/(k_{F,+}a_F) \approx 0.8$ for $m_r = 1$. However, in the extreme BEC limit [$1/(k_{F,+}a_F) \gg 1$], only the uniform superfluid phase exists even for $P < 0$ (not shown).

Next, we analyze gaussian fluctuations from which we extract the low frequency and long wavelength collective excitations at zero temperature. The collective excitation spectrum is determined by the poles of the propagator matrix $\mathbf{F}(q)$ determined by the condition $\det \mathbf{F}^{-1}(q) = 0$, when the usual analytic continuation $iv_\ell \rightarrow w + i0^+$ is performed. First, we express the fluctuation field as $\Lambda(q) = [\lambda(q) + i\theta(q)]/\sqrt{2}$, where $\lambda(q)$ and $\theta(q)$ are amplitude and phase fields, respectively. Then, we consider only the $P = 0$ or $k_{F,+} = k_{F,\uparrow} = k_{F,\downarrow}$ limit, and expand the matrix elements of $\mathbf{F}^{-1}(q)$ to second order in $|\mathbf{q}|$ and w to get

$$\mathbf{F}^{-1}(\mathbf{q}, w) = \begin{pmatrix} A + C|\mathbf{q}|^2 - Dw^2 & iBw \\ -iBw & Q|\mathbf{q}|^2 - Rw^2 \end{pmatrix}. \quad (7)$$

Thus, there are two branches for the collective excitations, but we focus only on the lowest energy one corresponding to the Goldstone mode with dispersion $w(\mathbf{q}) = v|\mathbf{q}|$, where $v = \sqrt{AQ/(AR + B^2)}$ is the speed of sound. Notice that extra care is required when $P \neq 0$ since Landau damping causes collective excitations to decay into

the two-quasiparticle continuum even for the s-wave case.

The BCS limit is characterized by the criteria $\mu_+ > 0$ and $\mu_+ \approx \epsilon_{F,+} \gg |\Delta_0|$. The expansion of the matrix elements to order $|\mathbf{q}|^2$ and w^2 is performed under the condition $[w, |\mathbf{q}|^2/(2m_+)] \ll |\Delta_0|$. The coefficient that couples phase and amplitude fields vanish ($B = 0$) in this limit. Thus, there is no mixing between the phase and amplitude modes. The zeroth order coefficient is $A = \mathcal{D}$, and the second order coefficients are $C = Q/3 = \mathcal{D}v_{F,\uparrow}v_{F,\downarrow}/(36|\Delta_0|^2)$, and $D = R/3 = \mathcal{D}/(12|\Delta_0|^2)$. Here, $v_{F,\sigma} = k_{F,\sigma}/m_\sigma$ is the Fermi velocity and $\mathcal{D} = m_+Vk_{F,+}/(2\pi^2)$ is the density of states per spin at the Fermi energy. Thus, we obtain $v = \sqrt{v_{F,\uparrow}v_{F,\downarrow}/3} = \sqrt{v_\uparrow v_\downarrow}$, with $v_\sigma = v_{F,\sigma}/\sqrt{3}$, which reduces to the Anderson-Bogoliubov relation when the masses are equal.

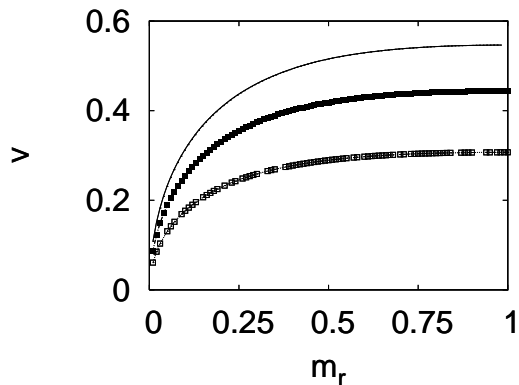


FIG. 4: Sound velocity v (in units of $v_{F,+} = k_{F,+}/m_+$) versus $m_r = m_\uparrow/m_\downarrow$ for $1/(k_{F,+}a_F) = -1$ (solid line), $1/(k_{F,+}a_F) = 0$ (solid squares) and $1/(k_{F,+}a_F) = 1$ (hollow squares). Here, populations are equal ($P = 0$).

On the other hand, the BEC limit is characterized by the criteria $\mu_+ < 0$ and $\xi_{\mathbf{k},+} \gg |\Delta_0|$. The expansion of the matrix elements to order $|\mathbf{q}|^2$ and w^2 is performed under the condition $[w, |\mathbf{q}|^2/(2m_+)] \ll |\mu_+|$. The coefficient $B \neq 0$ indicates that the amplitude and phase fields are mixed. The zeroth order coefficient is $A = \kappa|\Delta_0|^2/(2|\mu_+|)$, the first order coefficient is $B = \kappa$, and the second order coefficients are $C = Q = \kappa/[2(m_\uparrow + m_\downarrow)]$ and $D = R = \kappa/(8|\mu_+|)$, where $\kappa = \mathcal{D}/(32\sqrt{|\mu_+|\epsilon_{F,+}})$. Thus, we obtain $v = |\Delta_0|/\sqrt{4(m_\uparrow + m_\downarrow)|\mu_+|} = \sqrt{v_\uparrow v_\downarrow}$ with $v_\sigma = \sqrt{2\pi n_\sigma a_F/m_\sigma^2}$. Notice that the sound velocity is very small and its smallness is controlled by the scattering length a_F . Furthermore, in the theory of weakly interacting dilute Bose gas, the sound velocity is given by $v_B = \sqrt{4\pi a_{BB}n_B/m_B^2}$. Making the identification that the density of pairs is $n_B = n_+$, the mass of the bound pairs is $m_B = m_\uparrow + m_\downarrow$ and that the Bose scattering length is $a_{BB} = (m_B/m_+)a_F = [1 + m_\uparrow/(2m_\downarrow) + m_\downarrow/(2m_\uparrow)]a_F$, v_B reduces to the well known Bogoliubov relation when the masses are equal.

Therefore, the strongly interacting Fermi gas with two species can be described as a weakly interacting Bose gas at zero temperature as well as at finite temperatures [9]. Notice that a_{BB} reduces to $a_{BB} = 2a_F$ for equal masses [11] in the Born approximation, but a better estimate for a_{BB} can be found in the literature [12].

In Fig. 4, we show the sound velocity as a function of the mass ratio m_r for three values of the scattering parameter $1/(k_{F,+}a_F) = -1, 0$ and 1 corresponding to the BCS side [$1/(k_{F,+}a_F) = -1$], unitarity [$1/(k_{F,+}a_F) = 0$], and to the BEC side [$1/(k_{F,+}a_F) = 1$]. Notice that the speed of sound could be measured for a given m_r using similar techniques as in the single species case $m_r = 1$ [13, 14].

In summary, we analyzed the zero temperature phase diagram for an asymmetric two-component Fermi gas as a function of mass anisotropy and population imbalance. We identified regions corresponding to normal, and uniform or non-uniform superfluid phases, and discussed topological quantum phase transitions in the BCS, unitarity and BEC limits. Lastly, we derived the zero temperature low frequency and long wavelength collective excitation spectrum, and recovered the Bogoliubov relation for weakly interacting dilute bosons in the BEC limit. We thank NSF (DMR-0304380) for support.

Note added: We would like to acknowledge valuable e-mail correspondence with S.-K. Yip from June to August of 2006 in connection with differences and similarities between the stability criteria for the phase diagrams of the original versions of references [10] and [9] as well as of the present manuscript. In addition, recently, a few manuscripts have appeared addressing phase diagrams and their stability criteria for unequal population Fermi systems [15, 16, 17, 18, 19]. These manuscripts have led to a debate whether the compressibility criterion and the criterion based on the curvature of the thermodynamic potential with respect to the order parameter are equivalent or not. Our comments in connection to the current debate will be posted at a later date.

-
- [1] A. J. Leggett, in *Modern Trends in the Theory of Condensed Matter* (Springer-Verlag, Berlin 1980), p. 13.
 - [2] P. Nozieres and S. Schmitt-Rink, *J. Low. Temp. Phys.* **59**, 195 (1985).
 - [3] M. W. Zwierlein et al., *Science* **311**, 492 (2006).
 - [4] G. B. Partridge et al., *Science* **311**, 503 (2006).
 - [5] W. V. Liu and F. Wilczek, *Phys. Rev. Lett.* **90**, 047002 (2003).
 - [6] S. -T. Wu and S. -K. Yip, *Phys. Rev. A* **67**, 053603 (2003).
 - [7] P. F. Bedaque et al., *Phys. Rev. Lett.* **91**, 247002 (2003).
 - [8] L. He et al., *cond-mat/0604137*.
 - [9] M. Iskin and C. A. R. Sá de Melo, *cond-mat/0604184*.
 - [10] C. H. Pao et al., *cond-mat/0604572*.
 - [11] J. R. Engelbrecht et al., *Phys. Rev. B* **55**, 15153 (1997).

- [12] D. S. Petrov et al., *J. Phys. B: At. Mol. Opt. Phys.* **38**, S645 (2005).
- [13] J. Kinast et al., *Phys. Rev. Lett.* **94**, 170404 (2005).
- [14] M. Bartenstein et al., *Phys. Rev. Lett.* **92**, 203201 (2004).
- [15] L. Y. He et al., *cond-mat/0606322*.
- [16] E. Gubankova et al., *cond-mat/0603603*.
- [17] D. E. Sheehy and L. Radzihovsky, *cond-mat/0608172*.
- [18] Q. Chen et al., *cond-mat/0608454*.
- [19] C. H. Pao et al., *cond-mat/0608501*.